Phys. Status Solidi A **207**, No. 11, 2593–2596 (2010) / **DOI** 10.1002/pssa.201026270

physica status solidi a
www.pss-a.com
applications and materials science

Improvement of breakdown characteristics in AlGaN/GaN/$Al_xGa_{1-x}N$ HEMT based on a grading $Al_xGa_{1-x}N$ buffer layer

Hongbo Yu*[,1], Sefer B. Lisesivdin[1], Basar Bolukbas[1], Ozgur Kelekci[1], Mustafa Kemal Ozturk[2], Suleyman Ozcelik[2], Deniz Caliskan[1], Mustafa Ozturk[1], Huseyin Cakmak[1], Pakize Demirel[1], and Ekmel Ozbay[1,3]

[1] Nanotechnology Research Center, Bilkent University, Bilkent, 06800 Ankara, Turkey
[2] Department of Physics, Gazi University, 06500 Teknikokullar, Ankara, Turkey
[3] Department of Physics, and Department of Electrical and Electronics Engineering, Bilkent University, Bilkent, 06800 Ankara, Turkey

Received 23 May 2010, revised 2 July 2010, accepted 7 July 2010
Published online 3 August 2010

Keywords AlGaN, breakdown, GaN, heterostructures, high electron mobility transistors

* Corresponding author: e-mail yuhongbows@gmail.com, Phone: 90-312-290-1018, Fax: 90-312-290-1015

To improve the breakdown characteristics of an AlGaN/GaN based high electron mobility transistor (HEMT) for high voltage applications, AlGaN/GaN/$Al_xGa_{1-x}N$ double heterostructure (DH-HEMTs) were designed and fabricated by replacing the semi-insulating GaN buffer with content graded $Al_xGa_{1-x}N$ ($x = x_1 \rightarrow x_2$, $x_1 > x_2$), in turn linearly lowering the Al content x from $x_1 = 90\%$ to $x_2 = 5\%$ toward the front side GaN channel on a high temperature AlN buffer layer. The use of a highly resistive $Al_xGa_{1-x}N$ epilayer suppresses the parasitic conduction in the GaN buffer, and the band edge discontinuity limits the channel electrons spillover, thereby reducing leakage current and drain current collapse. In comparison with the conventional HEMT that use a semi-insulating GaN buffer, the fabricated DH-HEMT device with the same size presents a remarkable enhancement of the breakdown voltage.

© 2010 WILEY-VCH Verlag GmbH & Co. KGaA, Weinheim

1 Introduction Wide band gap AlGaN/GaN based high electron mobility transistors (HEMTs) are emerging as a promising candidate for high power, high voltage operations at microwave frequencies [1–7]. The application of AlGaN/GaN HEMT for power amplifiers requires off-state high breakdown voltages (V_{br}) for high power operation. Therefore, enhancing the V_{br} while keeping the gate–drain distance short is one of the most important challenges in the current developments of AlGaN/GaN based HEMT power devices. In the conventional AlGaN/GaN based HEMT epitaxial structure, the GaN is typically used as not only a buffer layer, but also the electron carrier channel. Because of the residual donors in undoped GaN, iron (Fe), or carbon (C) impurities were intentionally doped during the epitaxy growth in order to obtain a semi-insulating GaN buffer in the conventional AlGaN/GaN HEMT device. However, these technologies introduce deep-level defects in GaN layer, might cause memory effects and enhance the current collapse effect while applying high drain voltage [8, 9].

In our previous studies, we successfully developed undoped high crystalline quality GaN film with semi-insulating properties on high temperature AlN buffer [10, 11]. The fabricated HEMT device based on this semi-insulating GaN buffer showed a high device performance and good pinch-off characteristics [12]. In order to further improve the breakdown characteristics of the AlGaN/GaN HEMT device for high voltage applications, AlN and AlGaN become attractive alternatives over GaN as the buffer layer, which is due to their inherent material advantages: the wider energy band gap, higher breakdown fields, and superior confinement of sheet electron carriers [3–7].

In the present study, we designed and fabricated the AlGaN/GaN/$Al_xGa_{1-x}N$ grading layer ($x = x_1 \rightarrow x_2$, $x_1 > x_2$) based double heterostructure HEMT (DH-HEMT) by replacing the GaN buffer of the conventional HEMT with a thin Al content graded $Al_xGa_{1-x}N$ layer. Compared to the conventional AlGaN/GaN HEMT, the V_{br} of the fabricated DH-HEMT device was remarkably enhanced.

2 Experiment All of the AlGaN/GaN HEMT structures in the present study were grown on double polished c-plane sapphire by a low pressure MOCVD system. The

© 2010 WILEY-VCH Verlag GmbH & Co. KGaA, Weinheim

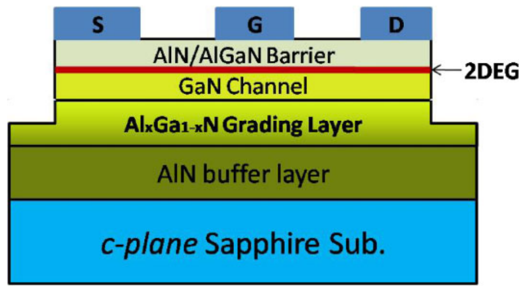

Figure 1 (online color at: www.pss-a.com) Schematic cross-sectional view of the fabricated AlGaN/GaN DH-HEMT with an Al content graded $Al_xGa_{1-x}N$ between the GaN channel and AlN buffer.

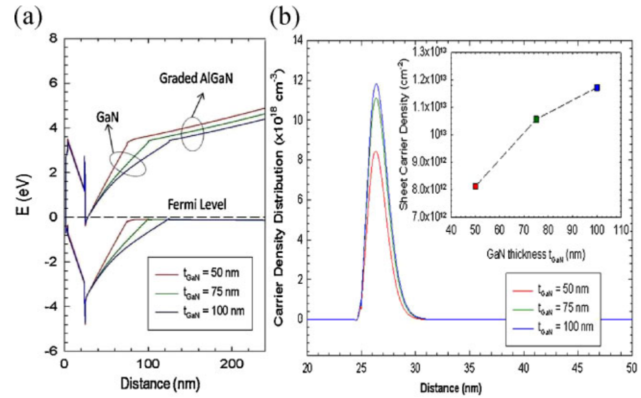

Figure 2 (online color at: www.pss-a.com) The simulated band diagram of several DH-HEMT structures with different thickness (50, 75, and 100 nm) of the GaN channel (a). Comparison of the carrier electrons distribution with a different GaN channel thickness (b).

cross-sectional schematic diagram of the fabricated DH-HEMT device is shown in Fig. 1. Firstly, a 0.5 μm-thick AlN film was grown on sapphire substrate, as described in the literatures [10–12]. The $Al_xGa_{1-x}N$ grading layer ($x = x_1 \rightarrow x_2$, $x_1 > x_2$) was then deposited by linearly lowering the Al composition x from $x_1 = 90\%$ to $x_2 = 5\%$ toward the front side on the high temperature AlN buffer layer.

Because the AlGaN alloy within an Al content of 10–90% has high thermal resistance [13], the thickness of the graded AlGaN layer was controlled to be as low as 250 nm. The 50 nm-thick GaN channel and AlN (1 nm)/$Al_{0.25}Ga_{0.75}N$ (20 nm) barrier layer were then deposited on the composition graded $Al_xGa_{1-x}N$ layer. All of the epitaxial layers in the HEMT structures are unintentionally doped. The DH-HEMT structure has the advantages of adopting the wide band gap from the AlN and graded $Al_xGa_{1-x}N$ buffer as well as the high electron mobility from the GaN channel together. For comparison, a conventional AlGaN/GaN based HEMT was grown using the same MOCVD reactor. In this conventional $Al_{0.25}Ga_{0.75}N$ (20 nm)/AlN (1 nm)/GaN HEMT, a 1.5 μm-thick semi-insulating GaN layer was grown directly on a high temperature AlN buffer without graded $Al_xGa_{1-x}N$, while the other layers in the two HEMT structures were consistent.

3 Results and discussion At room temperature (300 K), the Hall measurements of the conventional HEMT show a two-dimensional electron gas (2DEG) concentration and an electron mobility of $1.1 \times 10^{13}\,cm^{-2}$ and $1850\,cm^2\,V^{-1}\,s^{-1}$, respectively. While the proposed DH-HEMT epistructure exhibited a 2DEG concentration and an electron mobility of $8.3 \times 10^{12}\,cm^{-2}$ and $1260\,cm^2\,V^{-1}\,s^{-1}$, respectively. The sheet carrier density in the DH-HEMT can be further increased by the doping of the top $Al_{0.25}Ga_{0.75}N$ barrier, which does not deteriorate the electron confinement in the DH-HEMT structure. In our experiments, thick GaN directly grown on the high temperature AlN buffer was initiated from a three-dimensional (3D) growth mode. Then, the 3D island-like structure coalesces to a 2D smooth surface with the step-flow growth domination. By controlling the crystal coalescence process (the *in situ* reflectance from the onset of growth to fully recovered stable oscillations), it enables more of the edge-type TDs to annihilate by bending 90°, decreasing threading dislocation density in the GaN layer. However, in the DH-HEMT structure, the 3D to 2D growth process cannot be adopted due to the low GaN channel thickness. Therefore, the threading dislocations with high density in AlN buffer can probably be threaded all the way through the thin GaN channel. Compared to the conventional HEMT, the lower 2DEG mobility in the DH-HEMT structure might be due to the inferior crystalline quality of the thin GaN carrier channel (50 nm). The properties of the DH-HEMT are expected to be improved by reducing crystal defects in the high temperature AlN buffer layer.

Figure 2 shows the conceptual energy band diagrams for several different DH-HEMT structures, assuming that all the epitaxial layers have the Ga (or Al) crystal face. In all of the cases, the Al content in the top barrier layer is 25%, and in the bottom $Al_xGa_{1-x}N$ buffer layer, the Al content x is graded linearly from $x_1 = 90\%$ to $x_2 = 5\%$ toward the front side in a 250 nm thickness. All of the simulations contain an additional 10 Å AlN interlayer located between the $Al_{0.25}Ga_{0.75}N$ barrier and GaN channel in order to reduce alloy scattering. As shown in this figure, it is apparent that the spontaneous and piezoelectric polarization induced 2DEGs were formed at the $Al_{0.25}Ga_{0.75}N$ (barrier)/GaN (channel) interface. The GaN channel – $Al_{0.05}Ga_{0.95}N$ backside interface would have a conduction band off-set barrier ΔE_c of 0.06 eV to confine the carrier electrons. In addition, the confinement effect is enhanced by the gradually widening band gap toward the backside from the content graded $Al_xGa_{1-x}N$ buffer, which might further limit the electron spillover from the GaN channel and suppress the buffer leakage of the HEMT devices. The different curves in Fig. 2b show the effect of the thickness of the GaN channel between the AlN barrier and content graded $Al_xGa_{1-x}N$ bottom barrier layer. All of the layers are taken undoped. At the thin GaN channel layer (50 nm), the decrease of the spontaneous polarization induced carriers reduces the 2DEG density to

© 2010 WILEY-VCH Verlag GmbH & Co. KGaA, Weinheim

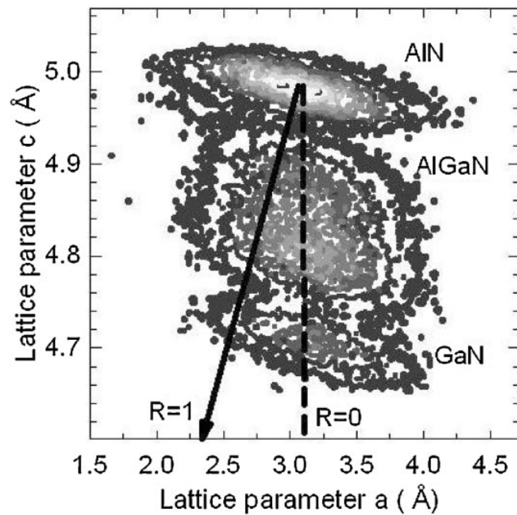

Figure 3 RSM around the asymmetrical (10−15) diffraction of the DH-HEMT structure with a composition graded $Al_xGa_{1-x}N$ layer between AlN under layer and the GaN channel. Full ($R=1$) and zero ($R=0$) relaxation lines are also shown.

$8.12\times10^{12}\,cm^{-2}$. With a thickness of the GaN channel increasing to 75 and 100 nm, the polarization induced sheet electron density is enhanced to 1.03×10^{13} and $1.15\times10^{13}\,cm^{-2}$, respectively.

The DH-HEMT epistructure was analyzed by high resolution X-ray diffraction (XRD). The XRD reciprocal lattice space mapping (RSM) was carried out around asymmetric (10−15) plane, which reveals the strain status in the epitaxial heterostructure. Figure 3 shows the (10−15) RSM of the XRD for the DH-HEMT epitaxial structure with 50 nm GaN channel, in which R is the strain relaxation factor. A value of $R=0$ corresponds to pseudomorphic strain accommodation, while $R=1$ indicates complete strain relaxation. As shown in this figure, the two domains corresponding to the AlN buffer and GaN channel are clearly separate. The domain of $Al_xGa_{1-x}N$ covers nearly throughout the AlN buffer to the GaN channel, corresponding to the epigrowth that the Al content is graded in a wide range from 90 to 5% in the $Al_xGa_{1-x}N$ alloy. The diffraction domain of an $Al_{0.25}Ga_{0.75}N$ barrier is located in the content graded $Al_xGa_{1-x}N$ buffer. Figure 3 shows that the domains of the GaN channel and the AlGaN epilayers are aligned to the domain of the AlN buffer layer along $R=0$ line, which demonstrates that the GaN channel and $Al_{0.25}Ga_{0.75}N$ barrier are coherently grown and fully strained to the graded $Al_xGa_{1-x}N$/AlN backside barrier in the DH-HEMT epistructure. Although the band gap widening in the content graded $Al_xGa_{1-x}N$ backside buffer would have a confinement effect on the sheet carrier, but also the content graded $Al_xGa_{1-x}N$ helps to resist the GaN relaxation on the AlN/sapphire system.

Sample HEMT devices were fabricated from the epistructures of conventional AlGaN/GaN HEMT and the proposed DH-HEMT. Ti/Al/Ni/Au (20:200:40:50 nm) was deposited for the source and drain Ohmic contacts that were annealed at 850 °C for 30 s under nitrogen atmosphere. The Ni/Au (40:100 nm) Schottky gates were then metalized. Reactive ion-etched mesa was performed for the device isolation. The gate length (L_G), gate width (W_G), distance between the source and drain (L_{SD}), and distance between the source and gate (L_{SG}) of the HEMT devices were 1, 250, 3, and 1 μm, respectively. Figure 4a compares the DC current–voltage (I_d–V_d) output characteristics of the two kinds of devices with the same size. When the gate bias was +1 V, the maximum drain current densities were measured as 705 and 510 mA mm^{-1} for the conventional HEMT (black square) and proposed DH-HEMT (red square frame), respectively. The pinch-off voltages for the conventional and DH-HEMT devices are −5 and −3 V, respectively. At the large drain biases and high current levels, negative differential resistance can be observed in both of the devices, which might be caused by the low thermal conductivity of sapphire substrate.

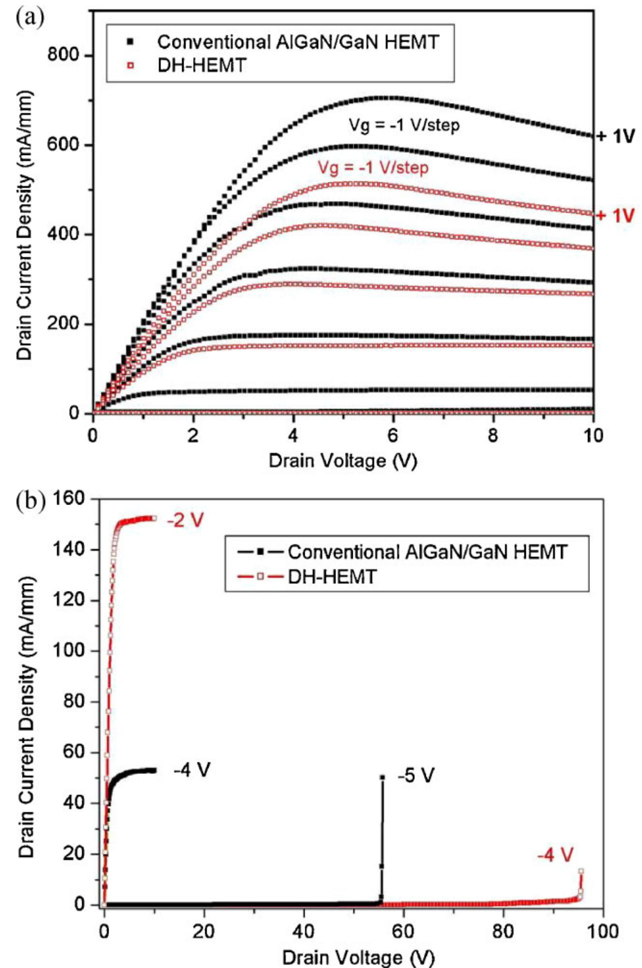

Figure 4 (online color at: www.pss-a.com) DC-IV output characteristics of a conventional AlGaN/GaN HEMT and a DH-HEMT (a) and (b) off-state DC-IV with a wide voltage range.

© 2010 WILEY-VCH Verlag GmbH & Co. KGaA, Weinheim

Figure 4b shows the off-state I_d–V_d curves in the two kinds of HEMT devices with wide V_d region. As shown in this figure, the fabricated conventional HEMT and DH-HEMT devices demonstrate sharp breakdown voltages of ~53 and ~95 V, respectively. The measurement results demonstrate that the breakdown characteristic of the DH-HEMT device is significantly improved compared to that of the conventional AlGaN/GaN HEMT. The DH-HEMT structure proposed in the present study is promising for the further higher power operation of high frequency applications.

In summary, to increase the breakdown voltage of the AlGaN/GaN HEMT for high voltage application, we designed and fabricated the DH-HEMT by replacing the GaN buffer with the Al content graded $Al_xGa_{1-x}N$ ($x = x_1 \rightarrow x_2$, $x_1 > x_2$) buffer by linearly lowering the Al content x from $x_1 = 90\%$ to $x_2 = 5\%$ toward the front side, which can significantly improve the carrier confinement and pinched-off behavior. Compared to the HEMT device using a conventional GaN buffer, the proposed DH-HEMT demonstrated a remarkable enhancement of the breakdown voltage.

Acknowledgements This work is supported by the European Union under the projects EU-PHOME, and EU-CONAM, and TUBITAK under Project nos. 107A004 and 107A012. One of the authors (E. O.) also acknowledges partial support from the Turkish Academy of Sciences.

References

[1] N. Q. Zhang, S. Keller, G. Parish, S. Heikman, S. P. DenBaars, and U. K. Mishra, IEEE Electron Device Lett. **21**, 421 (2000).
[2] W. Saito, M. Kuraguchi, Y. Takada, K. Tsuda, I. Omura, and T. Ogura, IEEE Trans. Electron Devices **51**, 1913 (2004).
[3] C. Q. Chen, J. P. Zhang, V. Adivarahan, A. Koudymov, H. Fatima, G. Simin, J. Yang, and M. A. Khan, Appl. Phys. Lett. **82**, 4593 (2003).
[4] K. Cheng, M. Leys, J. Derluyn, K. Balachander, S. Degroote, M. Germain, and G. Borghs, Phys. Status Solidi C **5**, 1600 (2008).
[5] N. Onojima, N. Hirose, T. Mimura, and T. Matsui, Jpn. J. Appl. Phys. **48**, 094502 (2009).
[6] T. Nanjo, M. Takeuchi, M. Suita, T. Oishi, Y. Abe, Y. Tokuda, and Y. Aoyagi, Appl. Phys. Lett. **92**, 263502 (2008).
[7] Z. Y. Fan, J. Li, M. L. Nakarmi, J. Y. Lin, and H. X. Jiang, Appl. Phys. Lett. **88**, 073513 (2006).
[8] S. Heikman, S. Keller, S. P. DenBaars, and U. K. Mishra, Appl. Phys. Lett. **81**, 439 (2002).
[9] S. Arulkumaran, T. Egawa, H. Ishikawa, and T. Jimbo, Appl. Phys. Lett. **81**, 3073 (2002).
[10] H. Yu, D. Caliskan, and E. Ozbay, J. Appl. Phys. **100**, 033501 (2006).
[11] S. Butun, M. Gokkavas, H. Yu, and E. Ozbay, Appl. Phys. Lett. **89**, 073503 (2006).
[12] H. Yu, M. K. Ozturk, S. Ozcelik, and E. Ozbay, J. Cryst. Growth **293**, 273 (2006).
[13] W. Liu and A. A. Balandin, J. Appl. Phys. **97**, 073710 (2005).

© 2010 WILEY-VCH Verlag GmbH & Co. KGaA, Weinheim